

## NATURAL-CONVECTIVE FLOW THROUGH A VERTICAL DUCT WITH A RESTRICTED ENTRY

J. R. DYER\*

The University of Adelaide, South Australia, 5001, Australia

(Received 9 August 1977 and in revised form 18 January 1978)

**Abstract**—This paper describes a study of laminar convective heat transfer to a fluid induced to flow by buoyancy forces through a heated vertical duct with a flow restriction at its lower end. The duct has a circular cross-section and the heating provides a uniform surface temperature. The entry restriction is formed by an unheated downward extension of the duct. The equations that govern the laminar natural-convective flow through the duct were solved by a step-by-step numerical technique. The relationship between the overall Nusselt number and the Rayleigh number is presented graphically in terms of the dimensionless flow rate and also in terms of the ratio of the unheated length of the duct to the heated length. This length ratio provides a measure of the severity of the entry restriction. An important finding of the study was that if the entry restriction exceeds a certain size, laminar upward flow throughout the whole of the heated part of the duct is not physically possible. This occurs if the ratio of the unheated length to the heated exceeds 18 for values of Rayleigh number up to 20 and exceeds only 2 for Rayleigh numbers in excess of  $10^3$ . Some experimental work was undertaken to corroborate the theoretical relationship and also to examine the nature of the flow in ducts for which the value of the unheated to heated length ratio for laminar flow throughout is exceeded.

### NOMENCLATURE

<p><math>a</math>, internal surface area of heated part of duct;</p> <p><math>c</math>, constant;</p> <p><math>c_p</math>, specific heat at constant pressure;</p> <p><math>g</math>, acceleration of gravity;</p> <p><math>Gr</math>, Grashof number, <math>g\beta(T_w - T_0)r_w^4/v^2l</math>;</p> <p><math>h_x</math>, heat dissipation rate from inlet to elevation <math>x</math>;</p> <p><math>H_x</math>, dimensionless heat dissipation rate from inlet to elevation <math>x</math>, <math>h_x/\rho c_p v l Gr(T_x - T_0)</math>;</p> <p><math>k</math>, thermal conductivity;</p> <p><math>l</math>, length of heated part of duct;</p> <p><math>L</math>, dimensionless length of heated part of duct, <math>l/Gr</math>;</p> <p><math>l_i</math>, length of unheated part of duct (entry restriction);</p> <p><math>L_i</math>, dimensionless length of unheated part of duct (entry restriction), <math>l_i/lGr</math>;</p> <p><math>Nu</math>, Nusselt number, <math>h_i r_w/a(T_w - T_0)k</math>, <math>h_i/2\pi l(T_w - T_0)k</math>;</p> <p><math>p</math>, pressure;</p> <p><math>P</math>, dimensionless pressure, <math>pr_w^4/\rho l^2 v^2 Gr^2</math>;</p> <p><math>p_d</math>, pressure defect (<math>p - p_0</math>);</p> <p><math>P_d</math>, dimensionless pressure defect, <math>p_d r_w^4/\rho l^2 v^2 Gr</math>;</p> <p><math>Pr</math>, Prandtl number, <math>\mu c_p/k</math>;</p> <p><math>q</math>, volume flow rate;</p> <p><math>Q</math>, dimensionless volume flow rate, <math>q/lvGr</math>;</p> <p><math>r</math>, radial co-ordinate;</p> <p><math>R</math>, dimensionless radial co-ordinate, <math>r/r_w</math>;</p> <p><math>Ra</math>, Rayleigh number, <math>GrPr</math>;</p> <p><math>Re_r</math>, Reynolds number (based on radius of duct), <math>u_m r_w/v</math>, <math>GrQl/\pi r_w</math>;</p>	<p><math>T</math>, temperature;</p> <p><math>u</math>, velocity in <math>x</math>-direction;</p> <p><math>U</math>, dimensionless velocity in <math>x</math>-direction, <math>ur_w^2/lvGr</math>;</p> <p><math>v</math>, velocity in <math>r</math>-direction;</p> <p><math>V</math>, dimensionless velocity in <math>R</math>-direction, <math>vr_w/v</math>;</p> <p><math>x</math>, vertical co-ordinate, <math>x = 0</math> at bottom of heated part of duct;</p> <p><math>X</math>, dimensionless vertical co-ordinate, <math>X = 0</math> at bottom of heated part of duct, <math>x/lGr</math>.</p> <p><b>Greek symbols</b></p> <p><math>\beta</math>, coefficient of thermal buoyancy;</p> <p><math>\theta</math>, dimensionless temperature, <math>(T - T_0)/(T_w - T_0)</math>;</p> <p><math>\mu</math>, dynamic viscosity;</p> <p><math>\nu</math>, kinematic viscosity;</p> <p><math>\rho</math>, density.</p> <p><b>Subscripts</b></p> <p><math>c</math>, centre line of duct;</p> <p><math>cx</math>, centre line of duct, elevation <math>x</math>;</p> <p><math>d</math>, defect (pressure);</p> <p><math>i</math>, unheated part of duct;</p> <p><math>m</math>, mean value;</p> <p><math>0</math>, ambient condition;</p> <p><math>opt</math>, optimum value;</p> <p><math>r</math>, radius of duct;</p> <p><math>t</math>, top of duct;</p> <p><math>w</math>, wall.</p>
---	---

### INTRODUCTION

WITH the growing need to conserve hydrocarbon energy resources, it is readily apparent that natural-convective systems are likely to find wider use in the future, particularly in domestic applications. For

\*Senior Lecturer, Department of Mechanical Engineering.

example, natural convection alone could provide the flow mechanism in some smaller types of solar heating and ventilating systems.

Since the work of Elenbaas [1, 2] was published in 1942, several papers on various aspects of natural-convective flow through open ended vertical ducts and channels have appeared in the literature [3–11]. One problem that has special relevance to natural-convective systems and yet has received little attention is the behaviour of natural-convective flow through a duct having a restricted-entry [5, 7, 11]. Clearly such a restriction will alter the behaviour of the flow within the duct and reduce the rate of heat transfer. For example, if the entry restriction is infinitely large, the duct will behave like an open thermosyphon [12]. (An open thermosyphon is a vertical duct that is closed at the bottom and open at the top.)

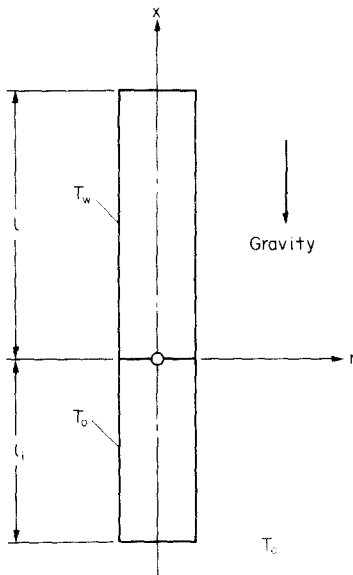


FIG. 1. Diagrammatic sketch of vertical circular duct with a restricted entry. The restriction is an unheated downward extension of the duct of length  $l_u$ .

The present paper describes an analytical and experimental investigation into the behaviour of the restricted-entry duct. The ducts considered were vertical and circular in cross-section. An entry restriction was provided, as shown in Fig. 1, by leaving the lower part of the duct unheated. This type of entry restriction was chosen because it produced, except if it were larger than a certain value, laminar flow in both the unheated and heated parts of the duct and thereby simplified the mathematical analysis. The heated wall of the duct was assumed to be at a uniform temperature and the unheated wall to be at ambient temperature.

A restricted-entry duct, as described above, can be classified for the purpose of heat transfer by two dimensionless parameters. First a modified Rayleigh number  $Ra$ , which is a conventional Rayleigh number (based on the radius of the duct  $r_w$ ) multiplied by the geometric parameter  $r_w/l$  (where  $l$  is the length of the heated part of the duct) and secondly, the ratio of the lengths of the unheated and heated parts,  $l_u/l$ .

## THEORETICAL CONSIDERATIONS

Heating the surface of the restricted entry vertical duct as shown in Fig. 1 will produce a natural-convective flow through the duct. In the following analysis it will be assumed that the flow is completely laminar and in an upward direction. This implies, as will be discussed later, that some limit is placed on the maximum value of the ratio of the unheated length to the heated,  $l_u/l$  for a given Rayleigh number. The additional simplifying assumptions that were made are: (a) the fluid is Newtonian; (b) fluid properties, except density, are independent of temperature; (c) density variations are significant only in producing the buoyancy force; (d) flow in the duct is steady, incompressible and axisymmetric.

The equations of continuity, momentum and energy in cylindrical co-ordinates for laminar flow are:

Continuity:

$$\frac{\partial u}{\partial x} + \frac{1}{r} \frac{\partial(rv)}{\partial r} = 0, \quad (1)$$

Momentum:

$$\rho \left[ u \frac{\partial u}{\partial x} + v \frac{\partial u}{\partial r} \right] = - \frac{\partial p}{\partial x} + \mu \left[ \frac{1}{r} \frac{\partial}{\partial r} \left( r \frac{\partial u}{\partial r} \right) + \frac{\partial^2 u}{\partial x^2} \right] - g\rho \quad (2)$$

$$\rho \left[ u \frac{\partial v}{\partial r} + v \frac{\partial v}{\partial r} \right] = - \frac{\partial p}{\partial r} + \mu \left\{ \frac{\partial}{\partial r} \left[ \frac{1}{r} \frac{\partial(rv)}{\partial r} \right] + \frac{\partial^2 v}{\partial x^2} \right\}. \quad (3)$$

Energy:

$$u \frac{\partial T}{\partial x} + v \frac{\partial T}{\partial r} = \frac{k}{\rho c_p} \left[ \frac{\partial^2 T}{\partial r^2} + \frac{1}{r} \frac{\partial T}{\partial r} + \frac{\partial^2 T}{\partial x^2} \right]. \quad (4)$$

Since the hydrostatic pressure of a fluid decreases with elevation according to the equation

$$\frac{dp_0}{dx} = -\rho_0 g \quad (5)$$

$[(\partial p_0/\partial x) + \rho_0 g]$  can be added to the RHS of the first momentum equation (equation 2). This yields

$$\rho \left[ u \frac{\partial u}{\partial x} + v \frac{\partial u}{\partial r} \right] = - \frac{\partial(p-p_0)}{\partial x} + \mu \left[ \frac{1}{r} \frac{\partial}{\partial r} \left( r \frac{\partial u}{\partial r} \right) + \frac{\partial^2 u}{\partial x^2} \right] + g(\rho_0 - \rho). \quad (6)$$

Expressing the buoyancy term in equation (6) in terms of the temperature difference  $(T - T_0)$ , and treating the pressure difference  $(p - p_0)$ , in the same equation as a pressure defect  $p_d$ , yields

$$\rho \left[ u \frac{\partial u}{\partial x} + v \frac{\partial u}{\partial r} \right] = - \frac{\partial p_d}{\partial x} + \mu \left[ \frac{1}{r} \frac{\partial}{\partial r} \left( r \frac{\partial u}{\partial r} \right) + \frac{\partial^2 u}{\partial x^2} \right] + \rho g \beta (T - T_0). \quad (7)$$

It is convenient to express equations (1), (3), (4) and (7) in dimensionless form. Radial dimensions are made dimensionless by referring them to the radius of the duct  $r_w$  and axial dimensions by referring them to the

product of the length of the duct  $l$  and the Grashof number  $Gr$ , that is,

$$R = r/r_w \text{ and } X = x/lGr. \tag{8}$$

It should be noted that generalising axial dimensions in this manner leads to the dimensionless length of the duct being given by

$$L = \frac{1}{Gr}. \tag{9}$$

This particular generalisation of the length of the duct [4] provides the basis, as will be seen later, for the method of solving the equations governing the flow. Using these dimensionless co-ordinates and the dimensionless variables listed in the Nomenclature, the dimensionless equations of continuity, momentum and energy, after eliminating small order terms, reduce to

$$\frac{\partial U}{\partial X} + \frac{V}{R} + \frac{\partial V}{\partial R} = 0 \tag{10}$$

$$U \frac{\partial U}{\partial X} + V \frac{\partial U}{\partial R} = - \frac{\partial P_d}{\partial X} + \frac{\partial^2 U}{\partial R^2} + \frac{1}{R} \frac{\partial U}{\partial R} + \theta \tag{11}$$

$$\frac{\partial P_d}{\partial R} = 0 \tag{12}$$

$$U \frac{\partial \theta}{\partial X} + V \frac{\partial \theta}{\partial R} = \frac{1}{Pr} \left[ \frac{\partial^2 \theta}{\partial R^2} + \frac{1}{R} \frac{\partial \theta}{\partial R} \right]. \tag{13}$$

Terms containing the factor  $r_w/lGr$  have been omitted from the foregoing dimensionless equations. This was permissible because in most practical situations this factor, which is raised to the second power, would be very much less than unity.

If the heating of the duct is such that the changes in the density of the fluid can be considered to be negligible (except in giving rise to the buoyancy forces), the dimensionless flow rate  $Q$ , which is given by

$$Q = 2\pi \int_0^1 U_x R \, dR \tag{14}$$

will be constant throughout the length of the duct. This equation (equation 14) together with equations (10)–(13) govern the natural-convective flow of the fluid through the duct.

*General Nusselt number relationship*

A Nusselt-number relationship in terms of dimensionless parameters can be established in the following manner. The Nusselt number pertaining to the duct is defined as

$$Nu = \frac{h_t r_w}{a(T_w - T_0)k} \tag{15}$$

where  $h_t$  is the rate at which the internal surface dissipates heat,  $r_w$  is the radius of the duct,  $a$  is the surface area of the heated length and  $(T_w - T_0)$  is the temperature excess of the surface. If  $h_t$  is expressed in terms of the dimensionless rate  $H_t$  (as defined in the

Nomenclature) and  $a$  is replaced by  $2\pi r_w l$  equation (15) becomes

$$Nu = \frac{Gr Pr H_t}{2\pi} \tag{16}$$

or

$$Nu = \frac{Ra H_t}{2\pi}. \tag{17}$$

Since the relationship between  $Nu$  and  $Ra$  alone is required, the governing equations (10)–(14) were solved to determine how  $H_t$  in equation (17) varies with  $Ra$ . These equations were solved for the following boundary conditions (Table 1).

Table 1. Boundary conditions

Location	$U$	$V$	$\theta$	$P_d$
$X = -L_t$ and $R = 1$	0	0	0	0
$X = -L_t$ and $1 < R \leq 0$	$Q/\pi$	0	0	0
$-L_t < X < 0$ and $R = 1$	0	0	0	<0
$-L_t < X < 0$ and $R = 0$	var.	0	0	<0
$0 \leq X < L$ and $R = 1$	0	0	1	<0
$0 \leq X < L$ and $R = 0$	var.	0	var.	<0
$X = L$ and $R = 1$	0	0	1	0
$X = L$ and $R = 0$	var.	0	var.	0

In Table 1 it will be seen that the pressure defect  $P_d$ , at the bottom of the duct has been assumed to be zero. This assumption is not strictly correct because it ignores for one thing the pressure drop that induces fluid at rest to flow to the inlet of the duct (namely,  $P_d = -U^2/2$  if a flat entry velocity profile is assumed). Aihara [9] demonstrated in the case of a duct formed by two parallel plates that ignoring the pressure drop at inlet, as hitherto [3–5], produced only a minimal effect on the computed relationship between the overall Nusselt number and the Rayleigh number. Likewise Dyer [10] later showed that in the case of a vertical circular duct dissipating a uniform heat flux the inclusion of the pressure drop at inlet in the computations had no effect on the overall Nusselt numbers at small Rayleigh numbers and reduced overall Nusselt numbers by less than 10% at large Rayleigh numbers. In view of these findings, together with the uncertainty about the actual flow pattern at inlet and the relatively large pressure drop that will occur in the unheated part of the duct, the pressure at inlet was taken to be zero.

At this point it is useful to consider some approximate Nusselt-number relationships, which can readily be derived, before beginning the general solution of the governing equations.

*Approximate Nusselt number relationship for small Rayleigh numbers (fully-developed flow)*

Small Rayleigh numbers can be obtained by making the length to radius ratio  $l/r_w$ , sufficiently large. With such a value of  $l/r_w$  the flow in the heated part of the duct will be fully developed, that is, the temperature of the fluid will be the same as that of the heated surface

and the velocity profile will be parabolic. Fully-developed flow can also be obtained in the unheated part of the duct by making  $l_i/r_w$  sufficiently large.

In this situation where both  $l$  and  $l_i \gg r_w$  and  $T \rightarrow T_w$  at  $x \ll l$ , the balance between the hydrostatic and viscous pressure differences is given by

$$\rho g \beta (T_w - T_0) l = \frac{32}{Re_r} \frac{(l_i + l)}{2r_w} \rho \frac{u_m^2}{2}. \quad (18)$$

Furthermore, the heat transferred to the fluid is

$$h_t = \rho q c_p (T_w - T_0). \quad (19)$$

Equations (18) and (19) yield

$$H_t = \frac{8}{\pi} Q^2 (1 + l_i/l). \quad (20)$$

It will be seen from equation (14) that for fully-developed flow  $H_t$  is equal to  $Q$  since  $\theta \rightarrow 1$ . Therefore from equation (20)

$$H_t = \frac{\pi}{8(1 + l_i/l)}. \quad (21)$$

Substituting equation (21) into equation (17) yields the following relationship for fully-developed flow:

$$Nu = \frac{Ra}{16(1 + l_i/l)}. \quad (22)$$

For a duct without an entry restriction (that is,  $l_i/l = 0$ ) equation (22) reduces to

$$Nu = \frac{Ra}{16}. \quad (23)$$

On the other hand, if  $l_i/l \rightarrow \infty$ ,  $Nu \rightarrow 0$  according to equation (22). This obviously would not be the case because heat would be dissipated by an open-thermosiphon flow that would occur in the upper part of the heated duct. It follows, therefore, that there will be a maximum value of  $l_i/l$  for upward flow throughout the duct.

#### *Approximate Nusselt-number relationship for large Rayleigh numbers (boundary-layer flow)*

Boundary-layer flow occurs in a duct that has a small value of  $l/r_w$  and consequently a large value of  $Ra$ . In this case temperature and velocity profiles near the surface of a relatively large diameter duct will be somewhat similar to those in the natural-convective boundary layer of a heated vertical flat surface. Consequently if the rates of heat transfer from both the duct and the flat surface are assumed to be similar, it follows that the Nusselt number of the duct has to be independent of the diameter. This condition is met by an equation of the form

$$Nu = cRa^{1/4} \quad (24)$$

from which the radius  $r_w$ , cancels out leaving  $l$  as the sole characteristic dimension. The value of  $c$  in equation (24) will be dependent upon  $l_i/l$ . For a plain-entry duct  $c$  would be approximately 0.6 [6, 7] and for restricted-entry ducts  $c$  should have smaller values. Furthermore, as in the case of the restricted-entry duct

with fully-developed flow, laminar upward flow throughout the duct will not be possible for all values of  $l_i/l$ .

#### *Solution of the flow equations*

In order to obtain the relationship  $Nu = f(Ra, l_i/l)$  for all laminar upward flow values of  $Ra$  and to study the development of the flow up the duct equations (10)–(14) were solved for the boundary conditions given previously by relaxation on a digital computer. As the present interest concerns uni-directional stream-wise flow, it was expedient to solve the equations by a step-by-step relaxation technique, the details of which have been described elsewhere [3, 4, 10, 11].

Each solution was computed for given values of the dimensionless flow rate  $Q$ , the dimensionless unheated length  $L_i$ , and the Prandtl number. A relaxation grid with 21 horizontal mesh points was superimposed on a radial plane through the duct. Each row up the duct was relaxed in turn for stream-wise and radial velocities, temperatures and the pressure defect. The solution was begun at the bottom of the duct where the entry velocity was assumed to be uniform. The unknown dimensionless heated length of the duct  $L$ , was established by continuing the relaxation up the duct until the pressure defect ceased to be negative. The reciprocal of the thus obtained dimensionless length  $L$ , by definition, gave the Grashof number. The dimensionless total heat-transfer rate  $H_t$ , was obtained from the following equation

$$H_t = 2\pi \int_0^1 U_i \theta_i R dR \quad (25)$$

and then the Nusselt number was found from equation (16).

Since air is the fluid in many natural-convective processes, the computations were carried out for a Prandtl number of 0.7. It is worth noting that computations for similar problems [10, 11] showed that the Prandtl number had only a very small effect on the relationship between Nusselt and Rayleigh numbers for  $Pr \geq 0.7$ . For smaller Prandtl numbers, however, quite the opposite was found to be the case.

#### *Theoretical results*

In Fig. 2 the computed Nusselt number of a duct for laminar flow throughout is presented as a function of the Rayleigh number and the dimensionless volume flow rate  $Q$ . The top curve describes the relationship for plain-entry ducts ( $l_i/l = 0$ ) and the curves for the various constant values of  $Q$  that branch off it are for restricted-entry ducts. In the fully-developed flow regime (associated with small values of  $Ra$ )  $Nu$  will be seen to be proportional to  $Ra$ . The explanation for this can be obtained by referring to equation (14) and (17). Since, as stated previously,  $Q$  and  $H_t$  for fully-developed flow will have the same value (which, according to equation (21), is dependent only upon the ratio  $l_i/l$ ), it follows from equation (17) that if  $Q$  is constant  $Nu$  will be proportional to  $Ra$ .

The  $Nu$ - $Ra$  relationship in a more practical form,

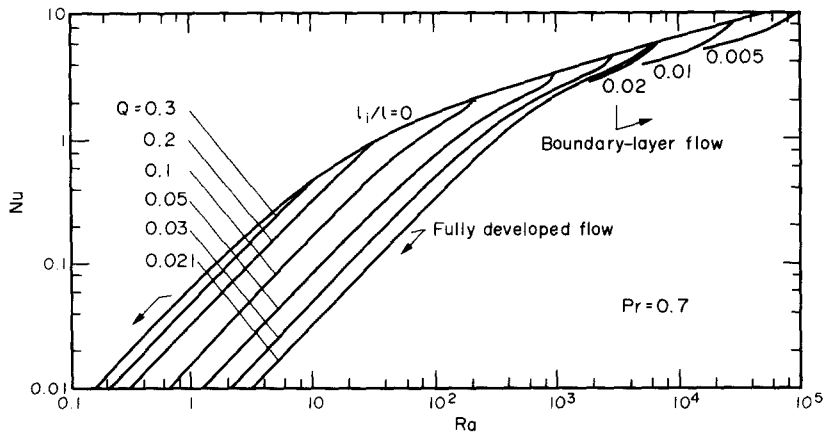


FIG. 2. Nusselt number vs Rayleigh number for laminar flow in restricted-entry ducts in terms of dimensionless flow volume,  $Q$ .

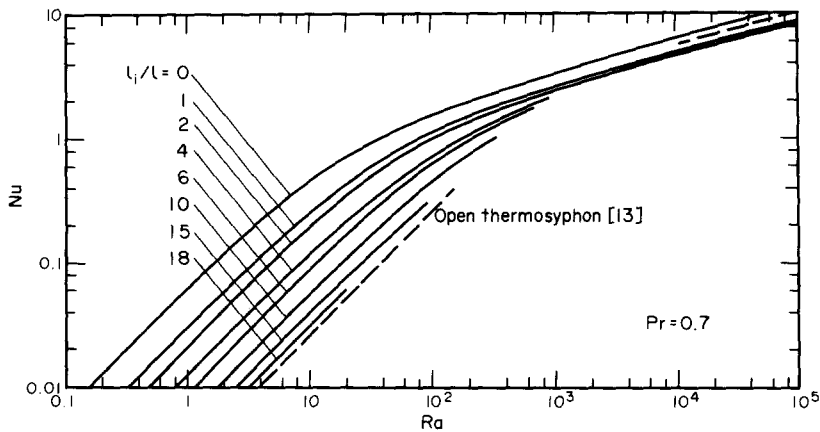


FIG. 3. Nusselt number vs Rayleigh number for laminar flow in restricted-entry ducts in terms of the unheated to heated length,  $l_i/l$ .

with  $l_i/l$  instead of  $Q$  as the third parameter, is shown in Fig. 3. This relationship will be seen to agree with equations (23) and (24), which were derived for fully-developed flow (small  $Ra$ ) and boundary-layer flow (large  $Ra$ ) respectively.

Returning to Fig. 2, a most interesting feature of the Nusselt-number relationship is that the computed  $Q$  curves for  $Q < 0.021$  actually terminate in the boundary-layer regime. This behaviour of the  $Q$  curves accounts for the fact in Fig. 3 that laminar upward flow throughout the duct is only possible if  $l_i/l \leq 18$  for small Rayleigh numbers and if  $l_i/l \leq 2$  for large Rayleigh numbers.

It can be deduced from Fig. 3 that the largest entry restriction that just allows upward flow reduces the value of  $Nu$  by a factor of 19 in the fully-developed flow regime and by a factor of only 1.3 in the boundary-layer flow regime. The Nusselt-number relationships for the two extreme conditions of fully-developed flow are:

$$Nu = \frac{Ra}{16} \text{ for } l_i/l = 0 \quad (26)$$

and

$$Nu = \frac{Ra}{304} \text{ for } l_i/l = 18. \quad (27)$$

These equations are in agreement with equation (23). The corresponding equations for the boundary-layer flow regime, which have the same form as equation (24), are

$$Nu = 0.63Ra^{0.25} \text{ for } l_i/l = 0 \quad (28)$$

and

$$Nu = 0.48Ra^{0.25} \text{ for } l_i/l = 2. \quad (29)$$

In Fig. 2 it will be recalled that the constant  $Q$  curves for  $Q \geq 0.021$  continue into the fully-developed flow regime. On the other hand, the curves that have values of  $Q$  less than 0.021 terminate in the boundary-layer regime. It was conjectured that the flow situation had changed when these points of termination were reached. To explain the phenomenon further, the temperature and velocity profiles in Figs. 4 and 5 for the continuous curve  $Q = 0.021$  will be examined. It will be seen in Fig. 4 that the velocity distribution for  $Ra$

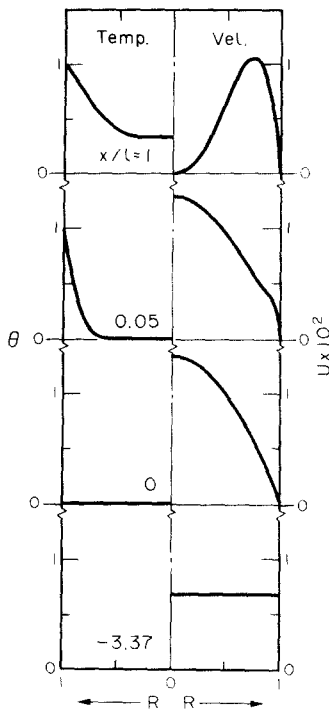


FIG. 4. Dimensionless temperature,  $\theta$  and velocity,  $U$  profiles for laminar flow in a restricted-entry duct in which the velocity on the centre line falls to zero at the top of the duct.  $Ra = 1180$ ,  $Pr = 0.7$ ,  $Q = 0.021$  and  $l_i/l = 3.37$ .

= 1180 changes from a fully-developed parabolic profile at the beginning of the heated part of the duct to a boundary-layer profile. Furthermore, at the top of the duct the velocity on the centre line has fallen to zero. Now the effect on the velocity and temperature profiles of reducing  $Ra$  to 64 and still maintaining the same value of  $Q$  (that is,  $Q = 0.021$ ) is shown in Fig. 5. Again the velocity profile is parabolic at the beginning of the heated length but in this case the boundary-layer profile with zero velocity on the centre line occurs near the bottom of the heated length at  $x/l = 0.05$ . Further up the duct velocities in the centre region begin to increase and fluid reaches the top of the duct with a fully-developed flow profile. If, on the other hand,  $Ra$  is raised above 1180 while  $Q$  is still maintained equal to 0.021, boundary-layer flow is produced similar to that shown in Fig. 4 except that the velocity on the centre line does not drop to zero at the top of the duct.

Consideration will now be given to a  $Q$  curve of a slightly smaller value, namely  $Q = 0.020$ , which according to Fig. 2 terminates at  $Ra = 2 \times 10^3$ . At this value of  $Ra$  the velocity profiles are similar to those already shown in Fig. 4 with the velocity on the centre line dropping to zero at the top of the duct. With the same value of  $Q$  of 0.020 and a larger entry restriction to give a smaller  $Ra$ , boundary-layer flow with zero velocity on the centre line was found to occur below the top of the duct. However, instead of the velocities in the centre region increasing above this point as they did for the curve  $Q = 0.021$ , as shown in Fig. 5, the solution ran out of control because the step-by-step

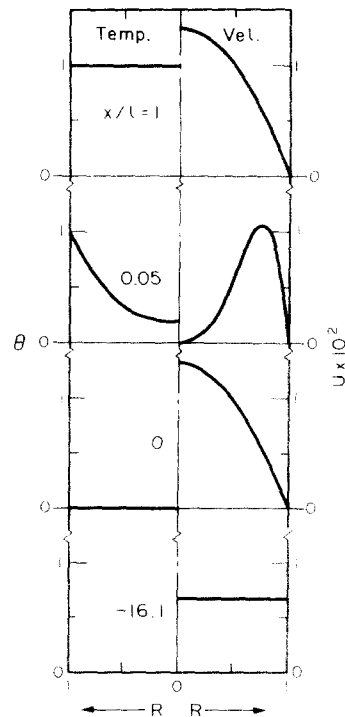


FIG. 5. Dimensionless temperature  $\theta$ , and velocity,  $U$  profiles for laminar flow in a restricted-entry duct in which the velocity on the centre line falls to zero and then increases again. The flow in the upper part of the duct is fully developed.  $Ra = 64$ ,  $Pr = 0.7$ ,  $Q = 0.021$  and  $l_i/l = 16.1$ .

relaxation will not handle other than uni-directional laminar-flow problems. It would appear, therefore, that the nature of the flow had changed owing to the cooler central region of the duct being no longer able to supply fluid to the growing boundary layer near the wall. This is in contrast to the previously discussed case of  $Q = 0.021$ ; here it was seen that the velocity on the centre line also fell to zero but thereafter it immediately began to increase because the temperature profile was more developed and consequently the boundary layer had ceased to grow.

Figure 6 shows the pressure defect along a restricted-entry duct for a small Rayleigh number. It will be observed that the pressure defect varies almost linearly in each part of the duct. This implies, of course, that the flow is fully developed.

It can be shown that a duct has a particular diameter for which the natural-convective rate of heat transfer per unit cross-sectional area is a maximum. To determine this optimum diameter it will be assumed that the heated length  $l$ , the unheated length ratio  $l_i/l$ , and the temperature excess of the surface of the heated part are all fixed. The optimum diameter of the duct is established by finding the value of  $Ra$  that maximises the total heat transfer per unit cross-sectional area ( $h_t/\pi r_w^2$ ). Expressing  $h_t$  in the foregoing expression in dimensionless form produces

$$\frac{h_t}{\pi r_w^2} = \frac{H_t Gr \rho c_p \nu l (T_w - T_0)}{\pi r_w^2} \quad (30)$$

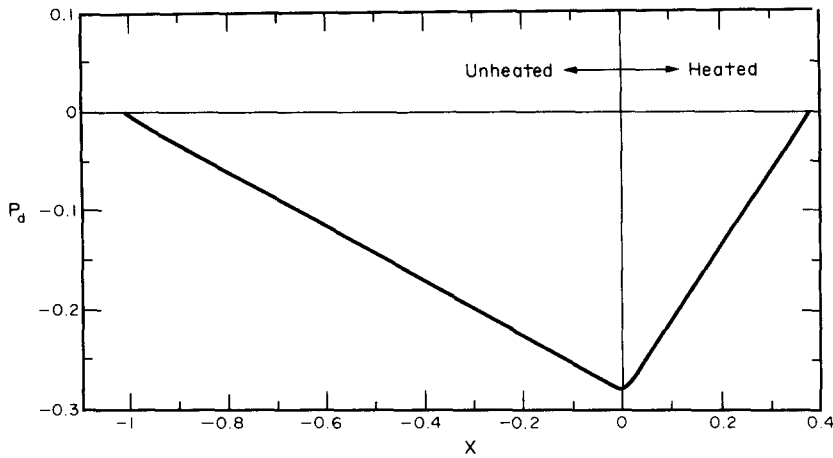


FIG. 6. The pressure defect along a restricted-entry duct in which the flow is laminar and essentially fully developed in both the restriction and the heated section.  $Ra = 1.8$ ,  $Pr = 0.7$ ,  $Q = 0.1$  and  $l_i/l = 2.6$ .

Using equation (16), equation (30) can be written as

$$\frac{h_i}{\pi r_w^2} = 2 \frac{Nu}{Pr} \frac{\rho c_p \nu l (T_w - T_0)}{r_w^2} \quad (31)$$

Multiplying the numerator and denominator on the RHS of equation (31) by  $Ra^{1/2}$  yields

$$\frac{h_i}{\pi r_w^2} = 2 \frac{Nu}{Ra^{1/2}} \rho c_p \left[ \frac{\beta g l (T_w - T_0)^3}{Pr} \right]^{1/2} \quad (32)$$

An inspection of equation (32) will show that for given values of  $l$  and  $(T_w - T_0)$  and for constant fluid properties the terms to the right of  $Nu/Ra^{1/2}$  are invariant. Hence it follows that

$$\frac{h_i}{\pi r_w^2} \propto \frac{Nu}{Ra^{1/2}} \quad (33)$$

This means that the heat transfer per unit cross-sectional area is proportional to  $Nu/Ra^{1/2}$  for given values of  $l$  and  $(T_w - T_0)$  and constant fluid properties. In Fig. 7, which shows a plot of  $Nu/Ra^{1/2}$  against  $Ra$ , it will be observed that  $Nu/Ra^{1/2}$  has a maximum value for a given  $l_i/l$ . Thus the optimum diameter of the duct can be obtained from the Rayleigh number that maximises  $Nu/Ra^{1/2}$  for the particular value of  $l_i/l$ . It

should be noted that for Prandtl numbers less than 0.7 the relationship between  $Nu/Ra^{1/2}$  and  $Ra$ , like that between  $Nu$  and  $Ra$ , becomes a strong function of the Prandtl number [11]. Consequently, data in Fig. 7 for determining the optimum diameter of a restricted-entry duct are valid only for  $Pr \geq 0.7$ .

EXPERIMENTAL STUDY

Equipment and procedure

Experiments were conducted, with air as the working fluid, to corroborate some of the theoretical findings and also to obtain information on ducts with larger entry restrictions than, as shown theoretically, would allow upward laminar flow to exist throughout the whole of the heated length. Three experimental ducts, the diameters of which were 25.4, 57.2 and 95.3 mm, were used; the heated length of each duct was 1220 mm.

Each duct was heated by three independent electrical resistance elements. The lengths of the elements and their winding pitches were designed to give a good approximation to a uniform surface temperature. The ducts were made of aluminium tubing with a wall thickness of 3.25 mm. The external surface of the 25.4 mm diameter duct was anodised and the bare nichrome wire heating elements were wound on to it (anodised aluminium is nonconducting at low voltages). However, in the case of the two larger diameter ducts grooves for locating the elements were turned on the outer surface before the tubes were anodised; as a precaution against short circuits at the edges of the grooves a layer of fibre glass tape was wrapped around the surface before the nichrome wire was wound on to the tube.

Fibre-glass insulation was wrapped around each duct to provide a heat-insulation wall, which was about 175 mm thick. Despite this large thickness of insulation the external heat loss was still significant and it had to be taken into account in a manner that will be described later.

The AC mains provided the power source for the heating elements. A voltage stabiliser was used to

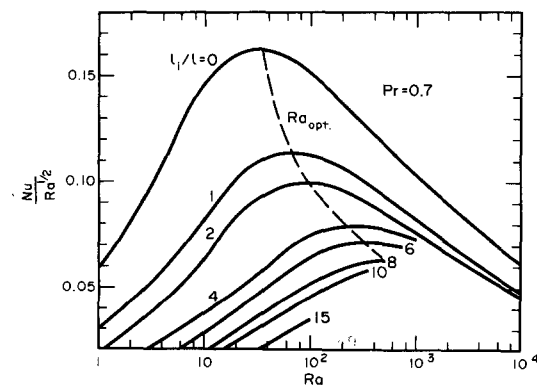


FIG. 7. Parameter  $Nu/Ra^{1/2}$ , which is proportional to the rate of heat transfer per unit flow area, vs Rayleigh number for restricted-entry ducts.

maintain a constant voltage across each element. The power supplied to each of the three heating elements was controlled by a variac.

Ideally the type of entry restriction should have been exactly the same as the one that was used in the theoretical model, that is, an unheated extension of the duct. However, as entry lengths of up to 150 times as long as the 1220 mm long heated tube were required, an obvious major accommodation problem was encountered. A compromise solution was adopted whereby the greater part of the pressure drop associated with  $l_i/l$  ratios in excess of unity occurred over a relatively short distance in a smaller diameter tube below a 975 mm long unheated tube of the appropriate diameter, which was attached to the bottom of the heated tube by a nylon coupling. This 975 mm long tube, in addition to providing an  $l_i/l$  ratio of 0.8 helped to smooth the flow before it entered the heated tube. Surface temperatures were monitored by nine thermocouples imbedded in the wall. A travelling thermocouple measured temperatures along the centre line of the duct. Owing to the slight resistance to the flow it imposed, this thermocouple was inserted after the heat transfer measurements had been taken. Interruption to the flow below the junction of the thermocouple was minimal.

The rate at which the internal surface of the duct dissipated heat was obtained by subtracting the heat loss through the insulation from the total power input to the heating elements. The relationship between the external heat loss and the internal surface temperature was established by operating the duct at various temperatures with the ends blocked and the bore filled with pieces of fibre-glass insulation to minimise internal air movements.

In most experiments the temperature difference between the internal surface of the duct and the ambient air was kept between 5 and 65°C. If the temperature differences were less than 5°C, small errors in the measurement of the temperatures of the ambient air and the internal surface could produce relatively large errors in the temperature difference and consequently in the values of  $Nu$  and  $Ra$ . On the other

hand, large temperature differences were also unsuitable for two reasons. First, large temperature differences violate the condition that density variations should be small and secondly, the rate of increase in  $Gr$  diminishes significantly with increasing temperature difference because the kinematic viscosity of air, which appears in the denominator of  $Gr$  to the second power, increases with temperature.

To carry out a test, it was important that the heated surface of the duct was at a uniform temperature and in equilibrium with its surroundings. Obtaining this condition could take as long as 6 h. This fact coupled with the requirement of a stable ambient temperature meant that only one set of results could be obtained in a day.

For evaluating the Nusselt and Rayleigh numbers, the air properties, except the coefficient of thermal buoyancy, were determined at the temperature of the surface of the duct. The coefficient of thermal buoyancy was taken to be the reciprocal of the absolute temperature of the air entering the duct.

#### Experimental results

*Unrestricted-entry ducts.* The experimental results for ducts with plain entries are presented in Fig. 8. It will be seen that these results compare satisfactorily with the theoretical relationship reproduced from Fig. 3. Furthermore, they are in agreement with the experimental studies of Elenbaas [2].

Visualisation studies with smoke revealed that for  $Ra$  in excess of  $10^3$  the out-flowing plume became less laminar in appearance. Hence, inspection of Fig. 8 will show that for some of the tests on the 57.2 mm diameter duct and for all the tests on the 95.3 mm diameter duct the flow was transitional. These findings are in accordance with the critical values of  $Ra$  that can be found as follows. The Reynolds number of the duct, based on the radius, can be expressed as

$$Re_r = \frac{RaQl}{\pi Pr r_w} \quad (34)$$

Equation (34) gives the following critical values of  $Ra$  if 1150 is taken to be the critical value of  $Re_r$  [15]:

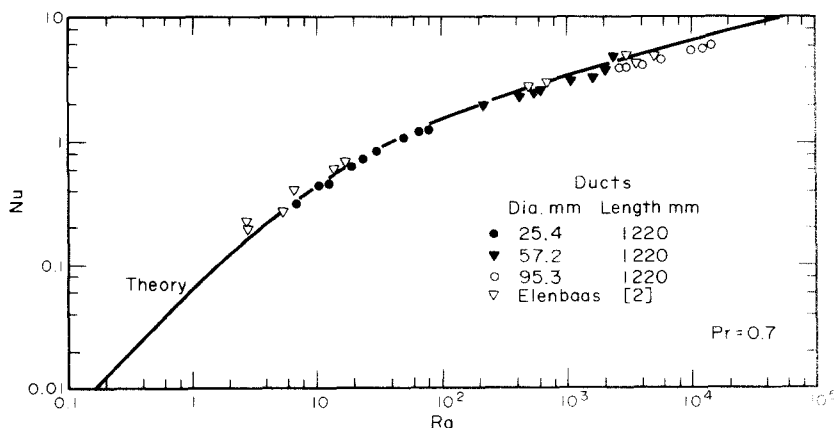


FIG. 8. Experimental Nusselt number vs Rayleigh number for ducts with no entry restriction ( $l_i/l = 0$ ) compared with the theoretical relationship.



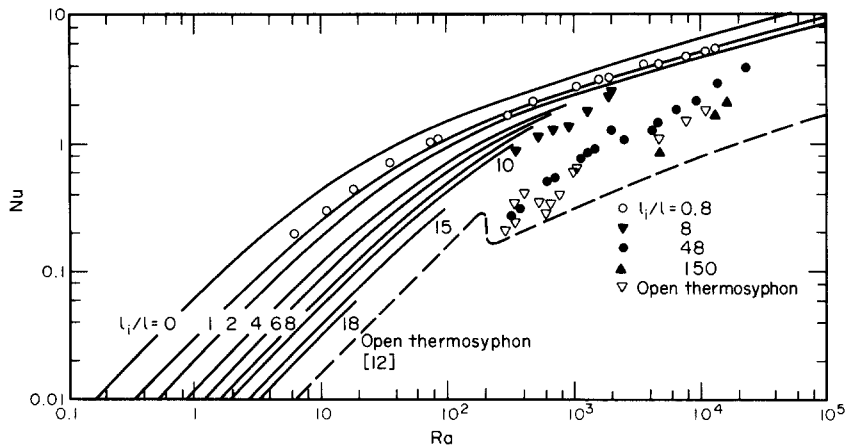


FIG. 9. Experimental Nusselt number vs Rayleigh number for restricted-entry ducts compared with the theoretical relationship for laminar upward flow throughout. Below  $Ra = 100$  the duct was 25.4 mm in diameter, between  $Ra = 2 \times 10^2$  and  $2 \times 10^3$  the duct was 57.2 mm in diameter and above  $Ra = 2 \times 10^3$  the duct was 95.3 mm in diameter. The heated length of each duct was 1220 mm. The experimental data on the open thermosyphon are in the impeding flow regime; the theoretical relationship shown is for  $Pr = 1$  and  $l/r_w = 50$  [12].

$3 \times 10^2$ ,  $2 \times 10^3$  and  $4 \times 10^3$  for the 25.4, 57.2 and 95.3 mm dia ducts respectively. (Owing to the less favourable shape of the velocity profile for boundary-layer flow, even smaller critical values of  $Ra$  could be expected.)

Although all the tests on the plain entry 25.4 mm dia duct yielded values of  $Ra$  below the critical value, it was surprising to find that temperatures measured along the centre line of the duct fluctuated significantly and in a random manner with the maximum intensity of fluctuation occurring about a third of the way up the duct. Temperature variations even greater than 10% of the temperature excess of the internal surface were recorded. In an attempt to explain this phenomenon, smoke carefully released near the entrance revealed that the air stream at entry was neither axisymmetric nor completely steady as hitherto assumed. It was decided, therefore, to provide the entry region with additional protection against stray air movements in the room. (As it was, the experiments were conducted in a closed room and within a draught shield.) The addition of a cylindrical shield, 180 mm in diameter and 200 mm deep, mounted on the underside of the duct was found to significantly reduce the temperature fluctuations and it was therefore concluded that the large temperature fluctuations were brought about by flow irregularities in the air as it entered the duct. This conclusion was reinforced by the fact that even with a small entry restriction ( $l_i/l = 0.8$ ) the smoothing of the air stream before it entered the heated length was such that the temperature fluctuations on the centre line were almost insignificant. Further evidence supporting this view was provided by solving the governing equations for arbitrary inlet velocity profiles. It was found that although the overall Nusselt number for a given Rayleigh number was relatively insensitive to the shape of the velocity profile at inlet, temperatures on the centre line differed by up to 8%.

*Restricted-entry ducts.* The heat-dissipation characteristics of restricted-entry ducts is shown in Fig. 9. The experiments with  $l_i/l = 0.8$ , which involved the three different diameter ducts, yielded results that agreed satisfactorily with the theory.

Rayleigh numbers in excess of 100 were chosen for investigating the behaviour of ducts with large values of  $l_i/l$ . This region was considered interesting because within it the theoretical Nusselt relationship for upward laminar flow tapers to a narrow band between  $l_i/l = 0$  and 2. Since, as previously mentioned, very long ducts could not be accommodated in the laboratory, a compromise was made whereby the greater part of the pressure drop over the entry restriction occurred in a smaller diameter tube below a 975 mm long tube of the appropriate diameter. This compromise, although it provided only approximate values of  $l_i/l$ , was justifiable on the ground that valuable information could be obtained, on which future work could be based. The estimation of the equivalent values of  $l_i/l$  was based on the fact that for a given laminar-flow rate the pressure drop across a tube (including the entrance effect) varies inversely with the fourth power of the diameter [15]. Although the tube of appropriate diameter between the smaller diameter tube and the heated duct was only 17 dia long for the 57.2 mm dia duct and 10 dia long for the 95.3 mm dia duct (a length of 20–40 dia would have been more desirable [15]), this was not considered to present a serious problem. As discussed previously, the theoretical overall Nusselt relationship was found to be relatively insensitive to the shape of the velocity profile at inlet and secondly, even with plain entry ducts unavoidable small flow irregularities at inlet were present.

Experimental results for the duct with  $l_i/l \sim 8$  yielded Nusselt numbers just below the theoretical Nusselt curves for upward laminar flow. The temperature of the out-flowing air was significantly higher than

Table 2. Temperature excess of the air leaving the duct on the centre line

$l_i/l$	$Ra$	$\frac{T_c - T_0}{T_w - T_0}$
0.8	1810	0.34
8	1910	0.82

that for the duct with  $l_i/l = 0.8$  at a similar Rayleigh number. This can be seen in Table 2.

The higher temperature excess of the air leaving the duct with  $l_i/l \sim 8$  implies that the flow would have acquired a certain degree of development. In other words, a value of  $(T_c - T_0)/(T_w - T_0)$  equal to 0.82 would not be consistent with a boundary-layer flow. If, as the theory predicted, a boundary-layer flow had developed in the lower part of the heated duct with the velocity on the centre line falling to zero, it is apparent that the flow rate in the central region would have increased again by some mechanism as the temperature of the air became more uniform across the duct. The nature of this mechanism will be discussed after the results for the duct with  $l_i/l \sim 48$  have been presented.

The results for the ducts with  $l_i/l \sim 48$ , are also plotted in Fig. 9. The slight discontinuity in the trend of the points that is noticeable at  $Ra = 2 \times 10^3$  marks the change from the 57.2 mm dia duct to the 95.3 mm dia. This discontinuity is attributed to errors associated with large temperature differences in the case of the smaller diameter duct and small temperature differences in the case of the larger diameter duct (see section on Equipment and procedure). The tests on the duct with  $l_i/l \sim 48$  revealed the following interesting phenomena.

1. The relative gap between the Nusselt number and that for the plain-entry duct decreased as the Rayleigh number increased. For example, at  $Ra = 2 \times 10^3$  the Nusselt number for  $l_i/l \sim 48$  is a factor of 4 below that for  $l_i/l = 0$ , whereas at  $Ra = 2 \times 10^4$  the Nusselt number for  $l_i/l = 48$  is a factor of only 2 lower. (A

similar trend was also apparent in the Nusselt numbers obtained from the duct with  $l_i/l \sim 8$ .) This pattern of increase in the Nusselt number for ducts with large entry restrictions is in contrast to the theoretical relationship for upward flow throughout the duct for Rayleigh numbers above  $10^3$ ; here the reduction factor for a given  $l_i/l$  is almost independent of the Rayleigh number.

2. Superimposed on the outflowing air from the duct with  $l_i/l \sim 48$  was an irregular flow into the duct. This flow was revealed by the careful release of smoke above the top of the duct. Further evidence of this was provided by the fluctuations in temperature just within the duct and by the lower mean temperatures compared with those further down the duct. These points are illustrated in Fig. 10. The irregular inward flow indicated, of course, that an open-thermosyphon effect had established itself in opposition to the weak flow up the duct.

3. Figure 10 also shows that the temperature along the centre line increased rapidly in the lower part of the duct. Temperatures, in fact, were very close to that of the wall between  $x/l = 0.37$  and 0.87. This implies, as in the case of the duct with  $l_i/l \sim 8$ , that the boundary-layer flow in the lower part of the duct had been superseded by a more developed laminar flow.

4. The large fluctuations in the temperature along the centre line up to  $x/l = 0.37$  should be noted in Fig. 10. These fluctuations, which are indicative of large scale, irregular air movements, could be associated in some way with the situation described in the Theoretical results where the central stream of cool fluid, owing to its low flow rate, could not meet the demands of the growing boundary layer near the wall. This point will be returned to later.

In order to study visually the flow produced by large entry restrictions a duct was made from clear perspex. This duct, which was intended to provide only qualitative data, had an internal diameter of 53 mm, a heated length of 857 mm and an unheated length of 1310 mm. A fine wire screen at the bottom provided the major resistance to flow.

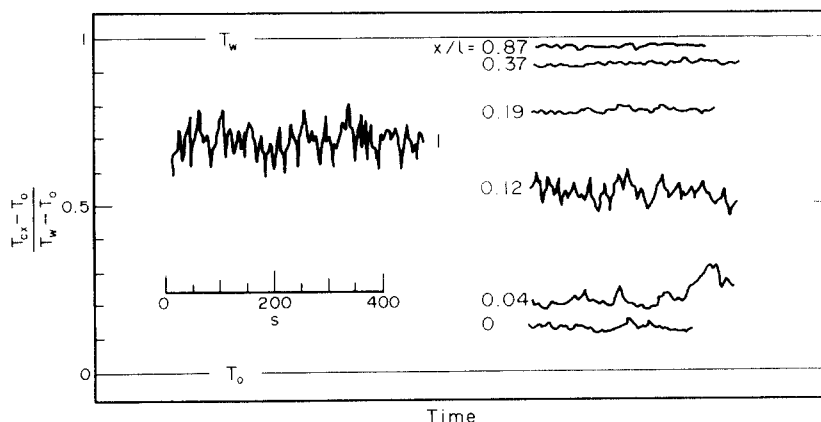


FIG. 10. Temperature fluctuations on the centre line of the 57.2 mm diameter restricted-entry duct. (Temperatures at each elevation were not recorded simultaneously.) The temperature at the top of the duct was depressed by the unsteady open-thermosyphon flow.  $Ra = 1040$ ,  $Pr = 0.7$ ,  $l_i/l \sim 48$ .

Smoke, generated by a draught-detecting device (manufactured by Auergesellschaft GMBH of Berlin), was released near the entrance to the duct. A distinctive laminar smoke plume developed in the unheated length but immediately it entered the heated length the smoke moved towards the wall. This was consistent with the growth of a strong boundary-layer flow as predicted in the theoretical work. After about 30 s the main volume of smoke passed out of the duct leaving a core of smoke (see Fig. 11) that stood away from the wall and was about 100 mm long. The bottom of the core was only 50–150 mm above the elevation at which heating began. Its actual position varied with the size

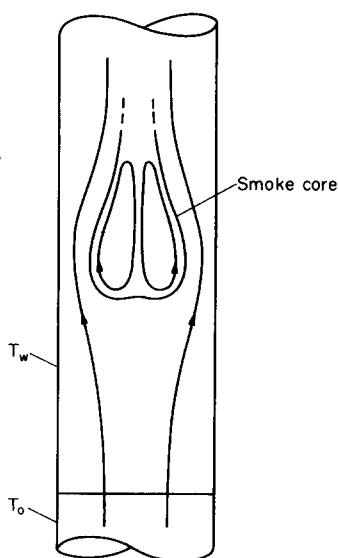


FIG. 11. Sketch of the core of smoke that remained in restricted-entry duct with a very large value of  $l_i/l$ . The inferred motion of the fluid around and within the core is superimposed.

of the restriction; the larger the restriction the lower the core was in the duct. Perhaps the most interesting thing about this core of smoke was that it was stable and remained visible up to 10 min after the smoke entered the duct. A symmetrical recirculation of air within the core is envisaged with the downward flow in the centre of it. Such a recirculatory motion could conceivably resolve the situation that developed when the central region could no longer supply enough fluid to the growing boundary layer. Above the recirculating flow it is likely that the temperature in the central region would have risen sufficiently to cause a reverse flow away from the wall towards the centre, thus leading to the growth of a developed laminar flow. The lower temperature fluctuations shown in Fig. 10 could have been caused by minor irregularities in the flow reacting with the recirculating flow. This point of view is strengthened by the fact that in tests when the wire screen at the bottom of the unheated portion of the duct was replaced by a smaller diameter tube, which would have produced a somewhat less favourable flow pattern, the lower surface of the smoke core showed signs of unsteadiness.

Tests on the largest diameter duct with  $l_i/l \sim 150$  yielded Nusselt numbers just below those for  $l_i/l \sim 48$ . An irregular open-thermosyphon flow at the top was again detected.

As the open-thermosyphon duct represents an extreme case of the restricted-entry duct (that is, one with an  $l_i/l$  ratio of infinity) the experimental ducts, although they were not specifically designed for the purpose, were operated as open thermosyphons by sealing their lower ends. The results of these tests, which agree reasonably well with the results of other workers [12–14], are also shown in Fig. 9. It should be noted that the Nusselt numbers for the two open thermosyphons and the restricted-entry ducts with  $l_i/l \sim 48$  and 150 lie in a fairly narrow band. Care must be taken, however, in interpreting the closeness of these results. First, the open thermosyphon for a given Rayleigh number is based on a smaller temperature excess of the wall because the outflowing air heats the space above the duct, which is the source of its coolant. Secondly, the small upward flow in a restricted-entry duct with a large value of  $l_i/l$  could upset the effectiveness of the open-thermosyphon flow that would otherwise establish itself in the upper part of the duct. And finally, two temperature excesses, it should be noted, are associated with those restricted-entry ducts that produce open-thermosyphon flows (in this experimental work the temperature of the air below the bottom of the duct was taken as the lower reference temperature). Likewise, Nusselt numbers for the open thermosyphons and the restricted-entry ducts cannot be directly compared because the temperature excess of the wall is also a parameter of the Nusselt number. These points are illustrated in Tables 3 and 4 where data are compared for an open thermosyphon and a restricted-entry duct that for similar Rayleigh numbers produced similar Nusselt numbers. Even with a value of  $l_i/l$  as large as 48 Table 4 shows that the restricted-entry duct still transferred the greater proportion of its heat in the lower part of the duct and consequently the upward flow of air was the major contributor to heat transfer.

#### CONCLUSIONS

This investigation has demonstrated that if an entry restriction is applied to a heated vertical duct of circular cross-section, the pattern of natural-convective flow through the duct can be significantly changed. The entry restriction that was used in the investigation was simply an unheated extension of the duct and the degree of restriction it imposed was expressed as the ratio of the unheated to the heated length,  $l_i/l$ . The theory showed the largest value of  $l_i/l$  that permitted upward laminar flow throughout the duct decreased from 18 in the fully-developed flow regime (small values of  $Ra$ ) to only 2 in the boundary-layer flow regime (large values of  $Ra$ ).

The heat transfer per unit cross-sectional area of a duct can be maximised. For a given heated length, a given temperature excess of the wall and specified fluid properties, the heat transfer per unit cross-sectional

Table 3. Comparison between the heat dissipated by a restricted-entry duct with  $l_i/l \sim 48$  and by an open-thermosyphon duct with a similar Rayleigh number; the ducts were 57.2 mm in diameter and the heated length of each was 1220 mm

	Restricted-entry duct $l_i/l \sim 48$	Open-thermosyphon duct
$Ra^*$	1040	1060
$Nu^*$	0.71	0.66
$T_w$ (°C)	44.4	102.2
$T_0$ (°C)	20.0	23.9
$T_{cr}$ (°C)	36.7	52.2
Temperature difference (°C)	$(T_w - T_0) = 24.4$	$(T_w - T_{cr}) = 50.0$
Heat dissipated (w)	3.72	7.77

\*The air properties, except the coefficient of thermal buoyancy, were evaluated at the temperature of the surface. The coefficient of thermal buoyancy was taken to be the reciprocal of the appropriate ambient absolute temperature.

Table 4. Comparison between a restricted entry duct and an open-thermosyphon duct with a similar Rayleigh number that shows the percentage of the total rate of heat transfer that was attributable to each heating element; the ducts were 57.2 mm in diameter and the heated length of each was 1220 mm

Height above the bottom of the heated length (mm)	Percentage of the total rate of heat transfer	
	Restricted-entry duct with $l_i/l \sim 48$ $Ra = 1040$	Open-thermosyphon duct $Ra = 1060$
911-1220	7	95
231-910	27	5
0-230	66	0
Total	100	100

area is maximised when  $Nu/Ra^{1/2}$  acquires its maximum value. The optimum Rayleigh number, and therefore the optimum diameter of the duct, is strongly influenced by the value of  $l_i/l$ .

For values of  $l_i/l$  larger than those shown in Fig. 3 for upward laminar flow throughout the duct, the boundary layer growing near the wall demanded more fluid than the cooler central region could supply and as a result the velocity on the centre line fell to zero. Velocity and temperature fields further up the duct could not be obtained from the step-by-step relaxation since this method of solution can handle only uni-directional flows.

The main thrust of the experimental work, therefore, was to obtain information on the behaviour of ducts with larger values of  $l_i/l$  than were predicted to give upward laminar flow throughout. Flow visualisation studies with smoke in such ducts revealed a core of air that overall did not move. Between this stationary core and the wall there was an upward flow. Within the core it is likely that there was a symmetrical recirculation with the down-flow in the centre region. This pattern of motion was probably the bridge between a growing boundary layer that could not be fed and the more

developed flow, associated with higher air temperatures, further up the duct.

If the value of  $l_i/l$  were sufficiently large, a weak, irregular open-thermosyphon flow established itself at the top of the duct in co-existence with the upward flow from the bottom. For Rayleigh numbers between  $2 \times 10^2$  and  $2 \times 10^4$  the restricted-entry ducts with  $l_i/l \sim 48$  and 150 and the open thermosyphons produced similar Nusselt numbers. However, owing to the temperature excess of the wall for a given Rayleigh number not being the same for the two types of duct, quite different rates of heat transfer were produced. This serves to emphasise that only in the limit does the restricted-entry duct approach the open thermosyphon in behaviour.

*Acknowledgements*—This investigation was carried out in the Department of Mechanical Engineering at The University of Adelaide. The author wishes to thank Professor R. E. Luxton, Dr. J. Mannam and Mr. J. H. Fowler for the valuable advice they gave on various aspects of the work. Also the help given by several students and the Mechanical Engineering Workshop in planning and carrying out the experimental investigation is gratefully acknowledged. Financial support for the project was provided by the Australian Institute of Nuclear Science and Engineering.

## REFERENCES

1. W. Elenbaas, Heat dissipation of parallel plates by free convection, *Physica, s'Grav.* **9**, 1–28 (1942).
2. W. Elenbaas, The dissipation of heat by free convection (from) the inner surface of vertical tubes of different shapes of cross-section, *Physica, s'Grav.* **9**, 865–874 (1942).
3. J. R. Bodoia, The finite difference analysis of confined viscous flow, Ph.D. Thesis, Carnegie Institute of Technology, Pittsburgh (1959).
4. J. R. Bodoia and F. J. Osterle, Development of free convection between heated vertical plates, *J. Heat Transfer* **84**, 40–44 (1962).
5. J. R. Dyer and J. H. Fowler, The development of natural convection in a partially-heated vertical channel formed by two parallel surfaces, *Mech. Chem. Engng Trans. Instn Engrs Aust.* **MC2**, 12–16 (1966).
6. J. R. Dyer, The development of natural convection in a vertical circular duct, *Mech. Chem. Engng Trans. Instn Engrs Aust.* **MC4**, 78–86 (1968).
7. J. R. Dyer, The development of laminar natural-convective flow in a vertical duct of circular cross-section that has a flow restriction at the bottom, in *Heat Transfer* 1970, Vol. 4, Paper NC2-8. Elsevier, Amsterdam (1970).
8. L. P. Davies and J. P. Perona, Development of free convection flow of a gas in a heated vertical open tube, *Int. J. Heat Mass Transfer* **14**, 889–903 (1971).
9. T. Aihara, Effects of inlet boundary-conditions on numerical solutions of free convection between vertical parallel plates, *Rep. Inst. High Speed Mech. Tohoku Univ.* **28**, 1–27 (1973).
10. J. R. Dyer, The development of laminar natural-convective flow in a vertical uniform heat flux duct, *Int. J. Heat Mass Transfer* **18**, 1455–1465 (1975).
11. J. R. Dyer, An investigation into the development of laminar natural convection in heated vertical ducts, Ph.D. Thesis, The University of Adelaide, Adelaide (1971).
12. M. J. Lighthill, Theoretical considerations on free convection in tubes, *Q. Jl. Mech. Appl. Math.* **6**, 398–439 (1953).
13. F. M. Leslie and B. W. Martin, Laminar flow in the open thermosyphon, with special reference to small Prandtl numbers, *J. Mech. Engng Sci.* **1**, 184–193 (1959).
14. B. W. Martin and H. Cohen, Heat transfer by free convection in an open thermosyphon tube, *Br. J. Appl. Phys.* **5**, 91–95 (1954).
15. E. C. R. Eckert and R. M. Drake, *Heat and Mass Transfer*, 2nd edn. McGraw-Hill, New York (1959).

CONVECTION NATURELLE DANS UNE COUDUITE VERTICALE  
AVEC UNE ENTREE FROIDE

**Résumé**—On étudie la convection naturelle laminaire dans une conduite verticale chauffée avec une restriction de l'écoulement à l'extrémité basse. La conduite a une section droite circulaire et le chauffage réalise une température de surface uniforme. La restriction à l'entrée est formée par une extension non chauffée du tube vers le bas. Les équations qui gouvernent l'écoulement à travers la conduite sont résolues par une technique numérique pas à pas. On présente graphiquement la relation entre le nombre de Nusselt global et le nombre de Rayleigh en fonction du débit adimensionnel du fluide et aussi en fonction du rapport de la longueur non chauffée à la longueur chauffée. Ce rapport de longueur fournit une mesure de la sévérité de la restriction d'entrée. Un résultat important de l'étude est que si la restriction d'entrée dépasse une certaine taille, l'écoulement laminaire ascendant dans la partie chauffée entière du tube n'est pas physiquement possible. Ceci se produit si le rapport de longueur dépasse 18 pour des valeurs du nombre de Rayleigh allant jusqu'à 20 et dépasse seulement 2 pour des nombres de Rayleigh supérieurs à  $10^3$ . Un travail expérimental partiel est conduit pour corroborer les résultats théoriques et aussi pour examiner la nature de l'écoulement dans les tubes pour lequel la valeur du rapport de longueur pour l'écoulement laminaire est dépassée.

FREIE KONVEKTIVE STRÖMUNG DURCH EINEN VERTIKALEN KANAL  
MIT BEHINDERTER ZUSTRÖMUNG

**Zusammenfassung**—Diese Arbeit beschreibt eine Untersuchung zur laminaren, konvektiven Wärmeübertragung an ein Fluid, das infolge Auftriebskräften durch einen beheizten vertikalen Kanal mit Behinderung der Zuströmung am unteren Ende strömt. Der Kanal hat einen kreisförmigen Querschnitt, und die Beheizung liefert eine gleichmäßige Oberflächentemperatur. Die Behinderung der Zuströmung wird durch eine unbeheizte Verlängerung des Kanals nach unten gebildet. Die Gleichungen, welche die laminare Strömung bei freier Konvektion durch den Kanal beschreiben, wurden ein schrittweises numerisches Verfahren gelöst. Die Beziehung zwischen der mittleren Nusselt-Zahl und der Rayleigh-Zahl wird in Abhängigkeit vom dimensionslosen Durchsatz und vom Verhältnis von unbeheizter zu beheizter Länge des Kanals grafisch dargestellt. Das Längenverhältnis liefert ein Maß für die Schwere der Zuströmungsbehinderung. Ein wichtiges Ergebnis der Untersuchung war, daß eine laminare Aufwärtsströmung im gesamten beheizten Teil des Kanals physikalisch nicht möglich ist, wenn die Behinderung ein gewisses Maß überschreitet. Dies passiert, wenn das Verhältnis von unbeheizter zu beheizter Länge bei Rayleigh-Zahlen bis 20 den Wert 18 und bei Rayleigh-Zahlen größer  $10^3$  nur den Wert 2 übersteigt. Einige experimentelle Versuche wurden unternommen, um die theoretische Beziehung zu bestätigen und auch um die Art der Strömung in Kanälen zu prüfen, bei denen das Verhältnis unbeheizter zu beheizter Länge die Werte für laminare Strömung im gesamten Bereich übersteigt.

### СВОБОДНОКОНВЕКТИВНОЕ ТЕЧЕНИЕ В ВЕРТИКАЛЬНОМ КАНАЛЕ С ПРЕДВКЛЮЧЕННЫМ НЕОБОГРЕВАЕМЫМ УЧАСТКОМ

**Аннотация** — В статье описывается теплообмен ламинарной естественной конвекцией в нагреваемом вертикальном канале с осложненными условиями течения на входе. Канал имеет круглое поперечное сечение с однородной температурой поверхности и входным дополнительным необогреваемым участком. Уравнения, описывающие ламинарное естественноконвективное течение в канале, решались численно. Графически представлено соотношение между средним числом Нуссельта и числом Рэлея, зависящее от безразмерной скорости и отношения длины необогреваемого участка к нагреваемому. Последнее соотношение определяет степень неоднородности граничных условий. Важным результатом исследования явилось наличие определенной длины участка, при которой ламинарный характер течения невозможен. Это наблюдается в том случае, если длина необогреваемого участка более чем в 18 раз превышает длину нагреваемого участка при значениях числа Рэлея не более 20 и только в 2 раза при значениях числа Рэлея больше  $10^3$ . Выполнен ряд экспериментов с целью подтверждения теоретических зависимостей и картины течения в каналах для ламинарного течения при различных значениях отношения длины необогреваемого участка к длине нагреваемого.